

P. BENNER  
S. GRUNDEL  
C. HIMPE  
C. HUCK  
T. STREUBEL  
C. TISCHENDORF

## **Gas Network Benchmark Models**

Preprint

Zuse Institute Berlin  
Takustr. 7  
14195 Berlin  
Germany

Telephone: +49 30-84185-0  
Telefax: +49 30-84185-125

E-mail: [bibliothek@zib.de](mailto:bibliothek@zib.de)  
URL: <http://www.zib.de>

ZIB-Report (Print) ISSN 1438-0064  
ZIB-Report (Internet) ISSN 2192-7782

# Gas Network Benchmark Models

P. Benner, S. Grundel, C. Himpe, C. Huck, T. Streubel, C. Tischendorf

**Abstract** The simulation of gas transportation networks becomes increasingly more important as its use-cases broadens to more complex applications. Classically, the purpose of the gas network was the transportation of predominantly natural gas from a supplier to the consumer for long-term scheduled volumes. With the rise of renewable energy sources, gas-fired power plants are often chosen to compensate for the fluctuating nature of the renewables, due to their on-demand power generation capability. Such an only short-term plannable supply and demand setting requires sophisticated simulations of the gas network prior to the dispatch to ensure the supply of all customers for a range of possible scenarios and to prevent damages to the gas network. In this work we describe the modelling of gas networks and present benchmark systems to test implementations and compare new or extended models.

---

Peter Benner

Max Planck Institute for Dynamics of Complex Technical Systems, Sandtorstr. 1, 39016 Magdeburg, Germany; e-mail: [benner@mpi-magdeburg.mpg.de](mailto:benner@mpi-magdeburg.mpg.de)

Sara Grundel

Max Planck Institute for Dynamics of Complex Technical Systems, Sandtorstr. 1, 39016 Magdeburg, Germany; e-mail: [grundel@mpi-magdeburg.mpg.de](mailto:grundel@mpi-magdeburg.mpg.de)

Christian Himpe

Max Planck Institute for Dynamics of Complex Technical Systems, Sandtorstr. 1, 39016 Magdeburg, Germany; e-mail: [himpe@mpi-magdeburg.mpg.de](mailto:himpe@mpi-magdeburg.mpg.de)

Christoph Huck

Department of Mathematics, Humboldt-Universität zu Berlin, Berlin, Germany; e-mail: [christoph.huck@math.hu-berlin.de](mailto:christoph.huck@math.hu-berlin.de)

Tom Streubel

Department of Optimization at Zuse Institute Berlin, Berlin, Germany and Department of Mathematics, Humboldt-Universität zu Berlin, Berlin, Germany; e-mail: [streubel@zib.de](mailto:streubel@zib.de)

Caren Tischendorf

Department of Mathematics, Humboldt-Universität zu Berlin, Berlin, Germany; e-mail: [tischendorf@math.hu-berlin.de](mailto:tischendorf@math.hu-berlin.de)

Symbol	Meaning	SI-Unit	Symbol	Meaning	SI-Unit
$\rho$	Density	$\left[\frac{\text{kg}}{\text{m}^3}\right]$	$R_s$	Specific gas constant	$\left[\frac{\text{m}^2}{\text{s}^2 \text{K}}\right]$
$p$	Pressure	$\left[\frac{\text{kg}}{\text{s}^2 \text{m}}\right]$	$\gamma$	Gas state	$\left[\frac{\text{m}^2}{\text{s}^2}\right]$
$\varphi$	Flow-rate	$\left[\frac{\text{m}^3}{\text{s}}\right]$	$z$	Compressibility factor	[1]
$q$	Mass-flow	$\left[\frac{\text{kg}}{\text{s}}\right]$	$S$	Cross-sectional area	$[\text{m}^2]$
$v$	Velocity	$\left[\frac{\text{m}}{\text{s}}\right]$	$D$	Pipe diameter	[m]
$g$	Gravity constant	$\left[\frac{\text{m}}{\text{s}^2}\right]$	$L$	Pipe length	[m]
$h$	Pipe elevation	[m]	$T$	Temperature	[K]
$\lambda$	Friction factor	[1]	$c$	Speed of sound	$\left[\frac{\text{m}}{\text{s}}\right]$
$R$	Gas constant	$\left[\frac{\text{kg m}^2}{\text{s}^2 \text{mol K}}\right]$	$P$	Power	[W]

**Table 1** List of Symbols

## 1 Introduction

The simulation of gas transport over large pipeline networks is essential to a safe and timely dispatch and delivery of contracted denominations. The modelling and verified implementation of gas transport is a prerequisite for the reliable simulation of gas transportation scenarios. Beyond the basic network of pipelines, further (active) components such as compressors have to be included into realistic models. To this end, a modelling approach for gas networks including these components is presented in this work together with four benchmark examples and associated reference solutions allowing the test of gas network simulation implementations.

The basis for gas network models are the Euler equations as introduced in [24], which describe the transient behavior in terms of conservation of momentum, conservation of mass and the gas state. Discretizations of this gas network model given by partial differential algebraic equations have been investigated in [6, 1]. An index reduction of this differential-algebraic model in a model order reduction setting has been investigated in [9, 11, 10]. The modelling of complex network elements such as compressors in the context of gas networks is described in [12, 7], while verification of this model has been conducted for example in [2, 25]. Modelling based on practical engineering considerations can be found in [8, 20].

In this work, we will present a modular gas network model based on the isothermal Euler equations. The modularity rests upon factor approximations which in different regimes are chosen accordingly. The focus of the modelling effort is hereby directed towards transient simulations of the gas transport. Beyond basic pipeline networks, the following modelling approach includes gas network elements like valves or compressors, and allows the extension with new elements. Additionally, certain benchmark networks are outlined together with respective scenarios, describing the transient boundary value behavior in order to provide testable discretized model instances.

In Section 2 we describe the model for a single pipe, which is extended to a network of pipes and additional components in Section 3. Section 4 details partial discretization of the network model and finally, Section 5 describes four benchmark networks with increasing degree of complexity.

## 2 Pipe Physics

### 2.1 The Isothermal Euler Equations

The flow of (a real) gas is modelled by the Euler equations, which describe the conservation of mass (1a), conservation of momentum (1b), and inherent state of the gas (1c). In the following, we discuss the analytic modelling, assumptions and simplifications of these partial differential equations (PDEs).

First of all, we assume that the temperature variations throughout the network have negligible effects on the dynamic behavior of the gas transport. This may seem unrealistic, but for strictly on-shore gas networks this actually is a sensible assumption [20, Ch. 45] and greatly reduces the complexity of the model. Hence, we fix the temperature to a constant value  $T_0$ .

For the transport of gas in a network of pipes, we first model a single pipe of length  $L$  by the one-dimensional isothermal Euler equations over the spatial domain  $x \in [0, L]$  and time  $t \in \mathbb{R}^+$ :

$$\frac{\partial}{\partial t} \rho = -\frac{\partial}{\partial x} \varphi, \quad (1a)$$

$$\frac{\partial}{\partial t} \varphi = -\frac{\partial}{\partial x} p - \frac{\partial}{\partial x} (\rho v^2) - g\rho \frac{\partial}{\partial x} h - \frac{\hat{\lambda}(\varphi)}{2D} \rho v |v|, \quad (1b)$$

$$p = \gamma(T) z(p, T) \rho. \quad (1c)$$

This system of coupled (PDEs) in space and time consists of the variables: density  $\rho = \rho(x, t)$ , flow rate  $\varphi = \varphi(x, t)$ , pressure  $p = p(x, t)$ , velocity  $v = v(x, t)$  and pipe elevation  $h = h(x)$ . Note, that the Euler equations are nonlinear (1b) and of hyperbolic nature [18].

The remaining components are: the gravity constant  $g$ , pipe diameter  $D$ , gas state  $\gamma(T)$ , friction factor  $\hat{\lambda}(\varphi)$  and the compressibility factor  $z(p, T)$ . The latter two functions will be discussed in Section 2.2 and Section 2.3. Also, as the temperature  $T$  is assumed constant, the temperature dependency of the gas state and compressibility factor is fixed to  $T \equiv T_0$ .

Subsequently we will transform this model, based on physical laws, to a representation which contains the measurable quantities as solution variables, to a more convenient form with respect to the numerical simulation. To this end we introduce the mass flow  $q = q(x, t) := m\varphi(x, t)$  and the pipe's cross-sectional area  $S := \frac{1}{2}D\pi^2$ , over which the gas flow in the pipe is averaged, to replace the velocity by mass flux (mass flow per area) over density  $v = \frac{1}{S} \frac{q}{\rho}$  and obtain:

$$\begin{array}{l}
\text{Pressure} \\
\text{(Continuity)} \\
\text{Mass Flux} \\
\text{(Momentum)}
\end{array}
\left\{ \begin{array}{l}
\frac{1}{\gamma_0} \frac{\partial}{\partial t} \frac{p}{z_0(p)} = -\frac{1}{S} \frac{\partial}{\partial x} q, \\
\frac{1}{S} \frac{\partial}{\partial t} q = -\frac{\partial}{\partial x} p - \underbrace{\frac{\gamma_0}{S^2} \frac{\partial}{\partial x} q^2 \frac{z_0(p)}{p}}_{\text{Inertia Term}} - \underbrace{\frac{g}{\gamma_0} \frac{p}{z_0(p)} \frac{\partial}{\partial x} h}_{\text{Gravity Term}} - \underbrace{\frac{\lambda(q)\gamma_0}{2DS^2} \frac{q|q|}{\left(\frac{p}{z_0(p)}\right)}}_{\text{Friction Term}}
\end{array} \right.$$

**Fig. 1** Term-wise highlighted PDE model with respect to physical meaning.

$$\frac{\partial}{\partial t} \rho = -\frac{1}{S} \frac{\partial}{\partial x} q, \quad (2a)$$

$$\frac{1}{S} \frac{\partial}{\partial t} q = -\frac{\partial}{\partial x} p - \frac{1}{S^2} \frac{\partial}{\partial x} \frac{q^2}{\rho} - g\rho \frac{\partial}{\partial x} h - \frac{\lambda(q)}{2DS^2} \frac{q|q|}{\rho}, \quad (2b)$$

$$p = \gamma(T)z(p, T)\rho. \quad (2c)$$

To match the change in variables, the friction factor is also adapted to the representation  $\lambda(q) := \hat{\lambda}(S\varphi)$ .

Using Boyle's Law and given the specific gas constant  $R_s$ , the gas state is constant  $\gamma_0 := \gamma(T_0) = R_s T_0$  and we define  $z_0(p) := z(p, T_0)$  due to the isothermality assumption. Finally, we substitute the pressure relation (2c) into (2a) and (2b) to obtain the following formulation of the isothermal Euler equations:

$$\frac{1}{\gamma_0} \frac{\partial}{\partial t} \frac{p}{z_0(p)} = -\frac{1}{S} \frac{\partial}{\partial x} q, \quad (3a)$$

$$\frac{1}{S} \frac{\partial}{\partial t} q = -\frac{\partial}{\partial x} p - \frac{\gamma_0}{S^2} \frac{\partial}{\partial x} q^2 \frac{z_0(p)}{p} - \frac{g}{\gamma_0} \frac{p}{z_0(p)} \frac{\partial}{\partial x} h - \frac{\lambda(q)\gamma_0}{2DS^2} \frac{q|q|}{\left(\frac{p}{z_0(p)}\right)}; \quad (3b)$$

see also Fig. 1.

The inertia (or kinematic) term of the mass-flux equation in the pipe gas flow model evolves on a much smaller scale compared to the other components [24]. This is justified by comparing the coupling term and the inertia term (first two right-hand side components in (3b)) after factoring the spatial derivative operator  $\frac{\partial}{\partial x}$ :

$$\left| \frac{\gamma_0}{S^2} \frac{q^2 z_0(p)}{p} \right| = \left| p \frac{v^2}{z_0(p)\gamma_0} \right| \ll |p|, \quad \text{for } z_0(p)\gamma_0 \gg v^2,$$

based on the velocity-mass-flux relation used in (2b). Since the speed of sound (in the medium)  $c \approx \sqrt{z_0(p)\gamma_0}$  typically exceeds the transport velocity  $v$ , the inertia term is discarded in several works, as i.e. [9, 11, 10, 13]. We will follow this approach and similarly exclude the inertia term from the model, which then leads to

$$\begin{aligned} \frac{\partial}{\partial t} \frac{p}{\gamma_0 z_0(p)} &= -\frac{1}{S} \frac{\partial}{\partial x} q, \\ \frac{\partial}{\partial t} q &= -S \frac{\partial}{\partial x} p - Sg \frac{p}{\gamma_0 z_0(p)} \frac{\partial}{\partial x} h - \frac{\lambda(q)}{2DS} \frac{q|q|}{\left(\frac{p}{\gamma_0 z_0(p)}\right)} \end{aligned} \quad (4)$$

The nonlinearity in the friction term  $\frac{q|q|}{p}$  may be treated as quadratic, i.e.  $\frac{q^2}{p}$ , only if the flow does not change direction. Since not only pipelines, but cyclic networks of pipes are considered, a flow direction may change throughout the course of a simulation. Some works [1, 28] linearize the friction term around the steady state of a given scenario, which is not considered in this work to preserve accuracy. Yet, the linearized equations may be used to obtain an approximate steady state given some boundary condition.

In terms of boundary conditions, the pressure and mass flow in the pipe at time  $t = 0$  as well as the pressure at the inflow boundary  $p_l(t) := p(0, t)$  and mass flow at the outflow  $q_r(t) := q(L, t)$  are given. With this set up, the aim is the computation of the pressure at the outflow boundary  $p_r(t) := p(L, t)$  and the mass flow at the inflow boundary  $q_l(t) := q(0, t)$ . Table 2 summarizes this relation of given boundary quantities and sought quantities of interest (QoI).

	Boundary	QoI
Pressure	$p(0, t)$	$p(L, t)$
Mass-Flux	$q(L, t)$	$q(0, t)$

**Table 2** Boundary values and quantities of interest.

It remains to be specified how the friction and compressibility factor are included into the model. As these factors are typically derived from formulas determined by experimental measurements, we will not specify which formula to use, but instead keep the model modular in this regard and present different popular choices for the aforementioned factors in the following.

## 2.2 Friction Factor

The friction factor  $\lambda(q)$  scales the (nonlinear) friction term and depends on the Reynolds number  $\text{Re}(q)$ , which in turn depends on the mass flow variable  $q$  for a flow in a pipe, and, depending on the approximation method, on the pipe roughness  $k$  and pipe diameter  $D$ . We will present two sets of approximation formulas for the friction factor (for turbulent flows): The first is predominately used in European countries, while the second is preferably used in the Commonwealth of Independent States (CIS) [20, Ch. 28]. In both regions, for a laminar flow (Reynolds numbers  $\text{Re} < 2100$ ), the well-known Hagen-Poiseuille formula is used to approximate the friction factor:

$$\lambda_{\text{HP}}(q) := \frac{64}{\text{Re}(q)}.$$

For Reynolds numbers  $\text{Re} > 4000$  a flow is considered turbulent. In the European region, the Colebrook-White formula [4], also known as Prandtl-Colebrook formula, is the most accurate approximation of the friction factor [29]:

$$\frac{1}{\sqrt{\lambda_{\text{CW}}(q)}} = -2 \log_{10} \left( \frac{2.51}{\text{Re}(q) \sqrt{\lambda_{\text{CW}}(q)}} + \frac{k}{3.71D} \right),$$

yet of implicit nature. An explicit variant of the Colebrook-White formula is given by the Hofer approximation [14]:

$$\lambda_{\text{H}}(q) := \left( -2 \log_{10} \left( \frac{4.518}{\text{Re}(q)} \log_{10} \left( \frac{\text{Re}(q)}{7} + \frac{k}{3.71D} \right) \right) \right)^{-2},$$

which is of sufficient accuracy for transient gas network simulations. The Nikuradse formula [23] results from the Hofer formula for  $\text{Re} \rightarrow \infty$ :

$$\lambda_{\text{N}}(q) := \left( -2 \log_{10} \left( \frac{k}{3.71D} \right) \right)^{-2}.$$

In the CIS region, approximations based on the Altschul formula [22, Ch. 7.26] are favored:

$$\lambda_{\text{A}}(q) := 0.11 \left( \frac{68}{\text{Re}(q)} + \frac{k}{D} \right)^{\frac{1}{4}}.$$

Similarly, for  $\text{Re} \rightarrow \infty$ , a simplified formula by Schiffrinson [20] exists:

$$\lambda_{\text{S}}(q) := 0.11 \left( \frac{k}{D} \right)^{\frac{1}{4}}.$$

Lastly, a simple yet commonly used approximation [19] of the friction factor for turbulent flows is given by the Chodanovich-Odischarija formula [3]:

$$\lambda_{\text{CO}}(q) := 0.067 \left( \frac{158}{\text{Re}(q)} + \frac{2k}{D} \right)^2.$$

### 2.3 Compressibility Factor

The inner state of the gas is described by (2c) and relates pressure, volume and temperature. To account for medium specific behavior deviating from an ideal gas, the compressibility factor  $z(p, T)$  is utilized. For an ideal gas, the compressibility factor is given independent from pressure and temperature by the unit constant:

$$z_1(p, T) := 1.$$

Typically, the compressibility factor is approximated using the Virial expansion:

$$z(p, T) = 1 + \sum_{k=1}^{\infty} B_k p^k,$$

for real gases. Usually, this expansion is truncated after the first terms, and the associated coefficients  $B_k$  are estimated heuristically. The AGA8-DC92 and SGERG [25] approximations are assembled in this fashion; see also [8]. Yet, the partial derivatives of the compressibility factor in (4) induce a root-finding problem due to the higher-order terms in the truncated series for these formulas. To avoid this additional complexity, we allow coarser but explicit approximations to the compressibility factor. Such explicit formulas for the compressibility factor are given first, by the AGA88 formula [17]:

$$z_2(p, T) := 1 + 0.257 \frac{p}{p_c} - 0.533 \frac{p T_c}{p_c T},$$

which is valid for pressures  $p < 70$  bar, and second, by the Papay formula [26]:

$$z_3(p, T) := 1 - 3.52 \frac{p}{p_c} e^{-2.26 \frac{T}{T_c}} + 0.247 \left( \frac{p}{p_c} \right)^2 e^{-1.878 \frac{T}{T_c}}.$$

The latter is valid up to  $p < 150$  bar and hence should be preferred due to the higher accuracy. The symbols  $p_c$  and  $T_c$  refer to the critical pressure and critical temperature, respectively. Since the temperature is assumed constant in this work, the compressibility factor formula  $z_2$  is a linear and  $z_3$  is a quadratic polynomial.

Since the previous obtained variant of Euler equations (4) requires derivatives of the compressibility factor with respect to pressure, these should be pre-computed analytically to prevent an on-demand numerical approximation.

### 3 Gas Network

The abstract gas transportation network is described by a directed graph:

$$\mathcal{G} = (\mathcal{N}, \mathcal{E}),$$

consisting of a tuple: A set of nodes  $\mathcal{N}$  and a set of oriented edges  $\mathcal{E}$ . The edges embody a (possibly large) number of pipes (P), as well as short pipes (S), valves (V), compressors (C), resistors (R), and controlled valves (CV). We introduce an index set  $\mathcal{I} = \{P, S, V, C, R, CV\}$  representing these components. Similarly, the nodes are divided into pressure nodes (p) and flux nodes (q), and we will create an index set for those as well  $\mathcal{J} = \{p, q\}$ . In total this means we can write the set of edges as a

union over the different components by using the corresponding index set. Likewise, this can be done for the set of nodes:

$$\begin{aligned}\mathcal{E} &= \mathcal{E}_P \cup \mathcal{E}_S \cup \mathcal{E}_V \cup \mathcal{E}_C \cup \mathcal{E}_R \cup \mathcal{E}_{CV} = \bigcup_{i \in \mathcal{I}} \mathcal{E}_i, \\ \mathcal{N} &= \mathcal{N}_p \cup \mathcal{N}_q = \bigcup_{j \in \mathcal{J}} \mathcal{N}_j.\end{aligned}$$

In the following we will repeat the set of equations used on each pipe and introduce the set of equations used for all other components.

### 3.1 Pipes

The Euler equation for the pressure  $p$  and the mass flux  $q$ , we use (4), depend on the following parameters that can vary for an individual pipe:

$$\gamma_0, z_0(p), S, h(x), \lambda(q), D. \quad (5)$$

Since a network consists of more than one pipe, we label the pressure and the flux function for each pipe by its pipe edge index  $e \in \mathcal{E}_P$ :  $p_e(x, t)$  and  $q_e(x, t)$  as well as all the parameters given in (5). The equations are then given by

$$\begin{aligned}\frac{\partial}{\partial t} d_{\text{pipe},e}(p_e) &= -\frac{1}{S_e} \frac{\partial}{\partial x} q_e, \quad \forall e \in \mathcal{E}_P \\ \frac{\partial}{\partial t} q_e &= -S_e \frac{\partial}{\partial x} p_e + f_{\text{pipe},e}(p_e, q_e), \quad \forall e \in \mathcal{E}_P\end{aligned} \quad (6)$$

where we also introduce the two nonlinear functions  $d_{\text{pipe},e}$  and  $f_{\text{pipe},e}$  for a simplified notation:

$$\begin{aligned}d_{\text{pipe},e}(p_e) &:= \frac{p_e}{\gamma_0^e z_0^e(p_e)}, \\ f_{\text{pipe},e}(p_e, q_e) &:= -S_e g_e d_{\text{pipe},e}(p_e) \frac{\partial}{\partial x} h_e - \frac{\lambda_e(q_e)}{2D_e S_e} \frac{q_e |q_e|}{d_{\text{pipe},e}(p_e)}.\end{aligned} \quad (7)$$

### 3.2 Non-Pipe Edge Components

We will give a short description of all the components used in the given benchmark models, namely the ones defined above: short pipe, valves, compressors, resistors

and controlled valves. For a comprehensive description of these and further gas network components, such as reservoirs or heaters, see also [8] and [20]. In order to describe these components we need four variables for each component, namely:  $p_{e,r}(t), p_{e,l}(t), q_{e,r}(t), q_{e,l}(t)$ , referring to the left and right pressure and the left and right flux for the edge  $e \in \mathcal{E}$ , meaning we work on a model that is discrete in space. For the sake of readability we will drop the time dependency in our notation (e.g.  $p_{e,l}$  instead of  $p_{e,l}(t)$ ) for the remainder of this section.

### 3.2.1 Short pipe

First, we introduce a short pipe element, which is an idealized network element with neither friction nor pressure loss due to height differences. The model is simply given by:

$$\begin{aligned} q_{e,r} - q_{e,l} &= 0, \\ p_{e,l} - p_{e,r} &= 0, \quad \forall e \in \mathcal{E}_S. \end{aligned} \quad (8)$$

### 3.2.2 Valves

Valves are gas network components, which connect two junctions and have two modes of operation: open and close. The open state means that the valve component acts as a pipe, while the closed state of the valve causes a disconnection of the junctions. Hence, the topology of the network can be changed if the valve is toggled between its two states, and thus significantly alter the behavior of the network for example by disconnecting a part of the graph or introducing cycles. A model for valves is given as follows:

$$\begin{cases} q_{e,r} = q_{e,l}, & p_{e,r} = p_{e,l} & \text{open valve} \\ q_{e,r} = q_{e,l} = 0 & & \text{closed valve} \end{cases} \quad \forall e \in \mathcal{E}_V. \quad (9)$$

According to this model, the adjacent nodes are topologically disconnected when the valve is closed, but connected by a short pipe otherwise.

### 3.2.3 Compressor/Ideal compressor unit

Compressors are complex gas network components which connect two junctions, and increase the energy (pressure) along the selected path. A basic model is given by the idealized compressor:

$$q_{e,r} = q_{e,l}, \quad (10a)$$

$$\frac{p_{e,r}}{p_{e,l}} = \alpha_{C,e}(p_{e,l}, p_{e,r}, q_{e,l}, q_{e,r}, t), \quad (10b)$$

where  $\alpha : \mathbb{R}^5 \rightarrow [1, \infty[$ . The model of the idealized compressor unit coincides with that of the short pipe whenever  $\alpha \equiv 1$ . So this may also serve as the minimum compression ratio provided by the idealized unit. We might also introduce more technical limitations to the capabilities of the ideal unit, e.g. by choosing a maximum compression ratio (e.g. 80bar/60bar). A further possibility might be a bound for power consumption. To this end, we solve the power equation from [8, eq. (2.43)] for the compression ratio  $p_{e,r}/p_{e,l} \equiv \alpha$  and substitute the power  $P$  by the maximum consumption allowed  $P_{\max}$ :

$$\alpha_{P,\max} \equiv \left[ \frac{\eta \cdot P_{\max}}{q_{e,r} \cdot R_s T_0 \cdot z_0(p_{e,l})} \cdot \frac{\gamma - 1}{\gamma} + 1 \right]^{\frac{\gamma}{\gamma - 1}}.$$

Here  $\gamma \eta \in ]0, 1[$  is a unit specific efficiency factor and is the isentropic expansion factor or isentropic exponent. The isentropic exponent corresponds to the ratio of specific heats for constant pressure and volume, and is the basis for isentropic processes such as idealized compression of (ideal) gas, which is based on the relation of pressure and volume before and after the compression  $p_{e,l} V_{e,l}^\gamma = p_{e,r} V_{e,r}^\gamma$  [8]<sup>1</sup>. By introducing target values  $p_{r,\text{set}}$  and  $p_{l,\text{set}}$  for the pressures, we can model two modes for  $\alpha$ :

$$\alpha_{C,e}(p_{e,l}, p_{e,r}, q_{e,l}, q_{e,r}, t) \equiv \begin{cases} \max \left( 1, \min \left( \frac{80}{60}, \alpha_{P,\max}, \frac{p_{r,\text{set}}}{p_{e,l}} \right) \right) & p_{r,\text{set}} \text{ mode} \\ \max \left( 1, \min \left( \frac{80}{60}, \alpha_{P,\max}, \frac{p_{e,r}}{p_{l,\text{set}}} \right) \right) & p_{l,\text{set}} \text{ mode} \end{cases}.$$

In either mode the idealized unit will try to keep the corresponding pressure value close to the *target value* ( $p_{r,\text{set}}$  or  $p_{l,\text{set}}$ ) w.r.t. to the modelled technical limitations.

Sometimes compressors consume some of the gas from the network to power themselves. Accordingly to [21] and [5], the fuel consumption can be modeled by replacing formula (10a) with:

$$q_{e,r} = q_{e,l} - \frac{d_c}{R_s T_0} c^2 \cdot q_{e,l} \left( \alpha_{C,e}(p_{e,l}, p_{e,r}, q_{e,l}, q_{e,r}, t)^{\frac{\gamma-1}{\gamma}} - 1 \right), \quad (11)$$

where  $d_c$  is a compressor specific constant.

### 3.2.4 Resistor

There is no existing infrastructure with the intended purpose of generating resistance. So *resistors* are virtual elements which resemble and substitute very local microscopic structures in our macroscopic view on a gas network. The following model of resistors is a simplified pipe model. This means we use some of the parameters used for the pipe as well. Here the friction and length parameter is replaced

<sup>1</sup> In [8] an approximation of  $\gamma = 1.296$  is used.

by a so called drag factor  $\xi$ . Height differences are neglected and time derivatives are set to zero:

$$q_{e,r} - q_{e,l} = 0, \quad p_{e,r} - p_{e,l} = -\xi \frac{R_s T_0 \cdot z_0(p_{e,r})}{2S_e^2} \frac{q_{e,l} |q_{e,l}|}{p_{e,r}}. \quad (12)$$

A very similar model is proposed in [8]. However the pressure on the right hand side of (12) is evaluated at the right boundary instead of the left. The reason for this subtle difference is that the resistor model (12) is derived consistently with the spatial discretization introduced later in Section 4.

### 3.2.5 Control valve

Control valves can be derived from the model (12) of resistors, but with a variable diameter. To that end we introduce a factor  $\alpha : \mathbb{R}^5 \rightarrow [0, 1]$ :

$$q_{e,r}(t) - q_{e,l}(t) = 0 \quad (13a)$$

$$\alpha_{CV,e}(p_{e,l}, p_{e,r}, q_{e,l}, q_{e,r}, t) \cdot (p_{e,r} - p_{e,l}) = -\xi \frac{R_s T_0 \cdot z_0(p_{e,r})}{2S_e^2} \frac{q_{e,l} |q_{e,l}|}{p_{e,r}}. \quad (13b)$$

Once again we may introduce target values for the ingoing and outgoing pressure and so we can model two modes via the degree of openness  $\alpha$ :

$$\alpha_{CV,e}(p_{e,l}, p_{e,r}, q_{e,l}, q_{e,r}, t) \equiv \begin{cases} \max\left(0, \min\left(1, -\xi \frac{R_s T_0 \cdot z_0(p_{r,\text{set}})}{2S_e^2 \cdot (p_{r,\text{set}} - p_{e,l})} \frac{q_{e,l} |q_{e,l}|}{p_{r,\text{set}}}\right)\right) & p_{r,\text{set}} \text{ mode} \\ \max\left(0, \min\left(1, -\xi \frac{R_s T_0 \cdot z_0(p_{e,r})}{2S_e^2 \cdot (p_{e,r} - p_{l,\text{set}})} \frac{q_{e,l} |q_{e,l}|}{p_{e,r}}\right)\right) & p_{l,\text{set}} \text{ mode} \end{cases}$$

### 3.2.6 Summary of non-pipe components

For each  $i \in \mathcal{S} \setminus p$  we introduce a function  $f_{i,e}$ , where  $e \in \mathcal{E}_i$ .

$$\begin{aligned} f_{S,e}(p_{e,l}, p_{e,r}, q_{e,l}, t) &= p_{e,r} - p_{e,l}, \\ f_{V,e}(p_{e,l}, p_{e,r}, q_{e,l}, t) &= \chi_e(t)(p_{e,r} - p_{e,l}) + (1 - \chi_e(t))q_{e,l}, \\ f_{C,e}(p_{e,l}, p_{e,r}, q_{e,l}, t) &= p_{e,r} - \alpha_{C,e}(p_{e,l}, p_{e,r}, q_{e,l}, t) \cdot p_{e,l} \\ f_{R,e}(p_{e,l}, p_{e,r}, q_{e,l}, t) &= S_e(p_{e,r} - p_{e,l}) + \xi \frac{R_s T_0 z_0(p_{e,r})}{2S_e} \frac{q_{e,l} |q_{e,l}|}{p_{e,r}}, \\ f_{CV,e}(p_{e,l}, p_{e,r}, q_{e,l}, t) &= \alpha_{CV,e}(p_{e,l}, p_{e,r}, q_{e,l}, q_{e,r}, t) \cdot (p_{e,r} - p_{e,l}) \\ &\quad + \xi \frac{R_s T_0 \cdot z_0(p_{e,r})}{2S_e^2} \frac{q_{e,l} |q_{e,l}|}{p_{e,r}} \end{aligned}$$

where  $\chi_e(t) = 1$  if the valve is open and  $\chi_e(t) = 0$  if the valve is closed. This means that we can write the equations for the components as:

$$\begin{aligned} q_{e,r} &= q_{e,l}, \\ 0 &= f_{i,e}(p_{e,l}, p_{e,r}, q_{e,l}, t) \quad e \in \mathcal{E}_i, i \in \mathcal{I} \setminus P. \end{aligned} \quad (14)$$

Thus we have a simple way to describe the equation on all edges.

### 3.3 Node conditions

We have a description of the pipe physics as a partial differential equation for the functions  $q_e(x, t)$  and  $p_e(x, t)$  for all  $e \in \mathcal{E}_p$ . Furthermore, we have two algebraic equations for the other components for the four variables  $q_{e,l}, q_{e,r}, p_{e,l}, p_{e,r}$ . Those four variables exist also for each pipe, namely:

$$q_{e,l}(t) = q_e(0, t), \quad q_{e,r}(t) = q_e(L_e, t), \quad p_{e,l}(t) = p_e(0, t), \quad p_{e,r}(t) = p_e(L_e, t),$$

where  $L_e$  is the length of the pipe  $e$ . We furthermore introduce the set of pressures  $p_u$  belonging to each node  $u \in \mathcal{N}$ . Describing the graph we distinguish between pressure nodes and flux nodes. At pressure nodes - as the name suggests - a pressure function is given:

$$p_u(t) = p_{\text{set}_u}(t), \quad u \in \mathcal{N}_p.$$

At the other nodes  $u \in \mathcal{N}_q$  the equations are modelled by a set of Kirchhoff-type balance equations:

$$\sum_{e \in \delta^-(u)} q_{e,r} - \sum_{e \in \delta^+(u)} q_{e,l}(t) = q_{\text{set}_u}(t), \quad u \in \mathcal{N}_q,$$

where  $\delta^+(u)$  and  $\delta^-(u)$  are sets of edges in which  $u$  is a right or left node, respectively. The functions  $p_{\text{set}_u}(t)$  and  $q_{\text{set}_u}(t)$  are given as time-dependent input functions to the system and are typically encoded in a given scenario. At nodes with neither in- nor outflow the function  $q_{\text{set}_u}(t)$  is set to zero. Sometimes the mass flow nodes are separated into ones with identically zero-set flow and those where that is not the case. The next condition connecting the different notation of the pressure will be eliminated in a further step of the description of the system. But for now, as we have left and right pressure for each edge as well as pressure on the node, we have to make sure these are consistent. This results in:

$$p_u = p_{e,l} \text{ and } p_v = p_{e,r} \quad \forall e = (u, v) \in \mathcal{E}.$$

### 3.4 Partial Differential Algebraic Equation

The overall so called Partial Differential Algebraic Equation (PDAE) is then given by:

$$\frac{\partial}{\partial t} d_{\text{pipe},e}(p_e) = -\frac{1}{S_e} \frac{\partial}{\partial x} q_e, \quad \forall e \in \mathcal{E}_P \quad (15)$$

$$\frac{\partial}{\partial t} q_e = -S_e \frac{\partial}{\partial x} p_e + f_{\text{pipe},e}(p_e, q_e) \quad \forall e \in \mathcal{E}_P \quad (16)$$

$$q_{e,l} = q_e(0, t) \quad q_{e,r} = q_e(L_e, t) \quad (17)$$

$$p_{e,l} = p_e(0, t) \quad p_{e,r} = p_e(L_e, t) \quad \forall e \in \mathcal{E}_P \quad (18)$$

$$q_{e,r} = q_{e,l}, \quad \forall e \in \mathcal{E}_i, i \in \mathcal{I} \setminus P \quad (19)$$

$$0 = f_{i,e}(p_{e,l}, p_{e,r}, q_{e,l}, t) \quad \forall e \in \mathcal{E}_i, i \in \mathcal{I} \setminus P \quad (20)$$

$$p_u(t) = p_{\text{set}_u}(t), \quad \forall u \in \mathcal{N}_P \quad (21)$$

$$\sum_{e \in \delta^-(u)} q_{e,r} - \sum_{e \in \delta^+(u)} q_{e,l}(t) = q_{\text{set}_u}(t), \quad \forall u \in \mathcal{N}_Q, \quad (22)$$

$$p_u = p_{e,l} \text{ and } p_v = p_{e,r} \quad \forall e \in \mathcal{E}, e = (u, v), u, v \in \mathcal{N} \quad (23)$$

In the system above we have the two PDE equations for each pipe describing the flow through the pipe (15, 16), then the definition of the boundary values for each pipe (17, 18). Then we have two equations for the nonpipe components. The first equation is (19) is the same for each component and the second equation (20) depends on the component specific function  $f_i$  for  $i \in \mathcal{I} \setminus P$ . Equation (21) defines the pressure at the pressure nodes and 22 the flow condition at the nodes where no pressure is given. The last equation (23) ensures that the different pressure variables at a given node do have the same value.

In order to be able to write this complex system in a concise form, we will first need to introduce the **incidence matrix** of a graph. Given a directed graph with  $N$  nodes and  $M$  edges, the associated incidence matrix  $A \in \mathbb{R}^{N \times M}$  is defined as:

$$A_{ij} := \begin{cases} 1 & \text{edge } j \text{ connects to node } i \\ 0 & \text{edge } j \text{ does not connect to node } i. \\ -1 & \text{edge } j \text{ connects from node } i \end{cases}$$

If this graph has a tree structure, meaning it is connected and acyclic, then the associated incidence matrix is of rank  $(N - 1)$  [11]. As we distinguish between different type of nodes and different types of edge we can always take only certain edges or nodes of the network and the incidence matrix that corresponds to the subgraph spanned by just those. For example, if we are interested in the incidence matrix for just pipes as edges and just the mass flow condition nodes we denote that matrix by  $A_{p,q}$ . Furthermore, we may only be interested in the negative part of the matrix or just in the positive part of that matrix. We call the negative matrix  $A^L$  and the positive  $A^R$  as the negative part represents the node to edge that connects on the left

to the matrix and the positive part corresponds to the node to edge relationship that connects on the right end of the edge. As before we can create submatrix in the same way.

The mass balance Kirchhoff type equation (22) can now be written as

$$A_q^R q_r + A_q^L q_l = q_{\text{set}}(t), \quad (24)$$

where  $q_r$  and  $q_l$  is a vector of all left and right flux for each edge. The equation 23 for the pressure reads

$$p_l = (A^L)^\top p, \quad p_r = (A^R)^\top p, \quad (25)$$

where the vectors  $p_r$  and  $p_l$  are as above and  $p$  is the vector of all pressures at the individual nodes.

Next, the spatial discretization for this partial differential algebraic equations is described, which then leads to a differential algebraic equation (DAE).

## 4 Discretization

To perform simulations of the partial differential algebraic equation modelling the gas flow in a network of pipes, the Euler equations in (4) need to be discretized. The considered model contains spatial  $\frac{\partial}{\partial x}$  and temporal  $\frac{\partial}{\partial t}$  derivative operators. We follow the established approach of discretizing first in space to obtain a differential-algebraic equation system, consisting of an ordinary differential equation system (in time) and a set of algebraic constraints. This will lead to an overall representation as an input-output system with the input-output quantities given in Table 2 for each supply node and demand node.

### 4.1 Spatial Discretization

#### 4.1.1 Spatial discretization of pipes

We present a spatial discretization of the pipe model (6) yielding index-1 DAEs for a stable integration if the pipes in the network are directed properly. Let  $e \in \mathcal{E}_P$  be an arbitrary edge modeling a pipe. As before, we introduce the discrete variables  $q_{e,l}(t) = q_e(0,t)$ ,  $q_{e,r}(t) = q_e(L_e,t)$ ,  $p_{e,l}(t) = p_e(0,t)$ ,  $p_{e,r}(t) = p_e(L_e,t)$  and discretize (6) spatially as follows:

$$\frac{d}{dt} d_{\text{pipe},e}(p_{e,l}(t)) + \frac{1}{S_e L_e} (q_{e,r}(t) - q_{e,l}(t)) = 0, \quad (26a)$$

$$\frac{d}{dt} q_{e,l}(t) + \frac{S_e}{L_e} (p_{e,r}(t) - p_{e,l}(t)) = f_{\text{pipe},e}(p_{e,r}(t), q_{e,l}(t)), \quad (26b)$$

with  $d_{\text{pipe}}$  and  $f_{\text{pipe}}$  defined by (7). The parameter  $L_e$  is the length of the pipe  $e$  and  $S_e$  is its diameter.

#### 4.1.2 Network DAE

We consider gas networks with network elements described in Section 3.2. Using the pipe discretization, we obtain a differential algebraic equation (DAE) of the form

$$E \frac{d}{dt} d(x(t)) + b(x(t), t) = 0.$$

Let  $p = (p_p, p_q)$  with  $p_p$  the pressure vector of the nodes with pressure conditions and  $p_q$  the ones without. Furthermore,  $q_{p,l}$  and  $q_{p,r}$  are the vectors of all pipe flows at left and right nodes of the pipes. Since the left and right flows of all non-pipe element models are equal, it is enough to consider only one flow per non-pipe arc. They are collected in a vector  $q_{\mathcal{A}}$ . Then the DAE is derived from the PDAE by replacing the first four equations (15)-(18) with (26), removing (19) by introducing just one variable for it and removing (23) by replacing  $p_l$  and  $p_r$  everywhere by equation (25). The equations (20)-(22) are written more concisely to get the following DAE:

$$\frac{d}{dt} d_{\text{pipe}}(A_{P,r}^\top p(t)) = D_S^{-1} D_L^{-1} (q_{P,l}(t) - q_{P,r}(t)) \quad (27a)$$

$$\frac{d}{dt} q_{P,l}(t) = -D_S D_L^{-1} (A_{P,r}^\top + A_{P,l}^\top) p(t) - f_{\text{pipe}}(A_{P,r}^\top p(t), q_{P,l}(t)) \quad (27b)$$

$$0 = f_{\mathcal{A}}(p(t), q_{\mathcal{A}}(t), t) \quad (27c)$$

$$0 = A_{P,r} q_{P,r}(t) + A_{P,l} q_{P,l}(t) + A_{\mathcal{A}} q_{\mathcal{A}}(t) - q_{\text{set}}(t) \quad (27d)$$

$$0 = p_p(t) - p_{\text{set}}(t). \quad (27e)$$

where  $d_{\text{pipe}}$  and  $f_{\text{pipe}}$  are vector-valued functions defined component-wise:  $(d_{\text{pipe}}(x))_e = (d_{\text{pipe},e})(x_e)$  and similar for  $f_{\text{pipe}}$ . For a concise notation we also introduce the constant diagonal matrices  $D_S$  and  $D_L$ :

$$D_S = \text{diag}\{S_e, e \in \mathcal{E}_P\} \quad D_L = \text{diag}\{L_e, e \in \mathcal{E}_P\}.$$

The algebraic element descriptions are given by

$$f_{\mathcal{A}}(p, q_{\mathcal{A}}, t) = [f_S, f_V, f_C, f_R, f_{CV}]^\top (A^L p, A^R p, q_{\mathcal{A}}, t),$$

with edge-wise defined functions  $f_i = (f_{i,e})_{e \in \mathcal{E}_i}$ ,  $i \in \mathcal{I} \setminus P$ .

In order to obtain a DAE system of index 1 for networks with a spatial pipe discretization of the form (26), one has to adapt the direction of pipes in the network to their topological location with respect to nodes with pressure and flow conditions.

#### Assumption 1

*Let a gas network with pipes, resistors and compressors be given and described by*

a graph  $\mathcal{G} = (\mathcal{N}, \mathcal{E})$  with the node set  $\mathcal{N}$  and the arc set  $\mathcal{E}$ . Denote the set of nodes with pressure conditions by  $\mathcal{N}_p$  and the set of pipe arcs by  $\mathcal{E}_p$ . Let  $\mathcal{N}_{\mathcal{A}}$  be the set of nodes  $u \in \mathcal{N} \setminus \mathcal{N}_p$  that have an arc  $e \in \mathcal{E} \setminus \mathcal{E}_p$  directing to  $u$ . The graph  $\mathcal{G}$  shall fulfill the following conditions:

1. Each pipe  $e^p$  is connected to a node of  $\mathcal{N} \setminus (\mathcal{N}_p \cup \mathcal{N}_{\mathcal{A}})$ .
2. Each connected component of  $\mathcal{G}_{\mathcal{P}} := (\mathcal{N}, \mathcal{E}_p)$  has at least one node in  $\mathcal{N}_p \cup \mathcal{N}_{\mathcal{A}}$ .
3. For each node  $u \in \mathcal{N}$ , there exists at most one arc in  $\mathcal{E} \setminus \mathcal{E}_p$  directing to  $u$ .
4. No arc of  $\mathcal{E} \setminus \mathcal{E}_p$  directs to a node of  $\mathcal{N}_p$ .

In this assumption we consider nodes that are connected to an arc that is not a pipe as special nodes and call the set of all these nodes by  $\mathcal{N}_{\mathcal{A}}$ . We assume that a pipe arc is always connected to a least one node that is not such a node and not a supply node. The second point in the assumption is that in each connected component of the network, we have a least one node that is either a supply node or connected to a non-pipe arc. The third point is that every node is the end node for at most one non-pipe arc and a non-pipe arc can never end in a supply node.

In [15] it has been shown that under these assumptions, the pipes of such gas networks can be directed in such a way that the resulting DAE formed by (27) has index 1 as the next theorem explains.

**Theorem 1.**

Let  $\mathcal{G} = (\mathcal{N}, \mathcal{E})$  be a connected, directed graph describing a gas network that fulfills Assumption 1. Then, the pipes in  $\mathcal{G}$  can be directed in such a way that

1. no arc directs to a node of  $\mathcal{N}_p$ ,
2. for each node  $u \in \mathcal{N} \setminus \mathcal{N}_p$ , there exists an arc directed to  $u$ ,
3. if an arc  $e \in \mathcal{E} \setminus \mathcal{E}_p$  directs to  $u \in \mathcal{N} \setminus \mathcal{N}_p$  then none of the arcs of  $\mathcal{E}_p$  is directed to  $u$

and the DAE formed by (27) has index 1.

Given a network, we set up the directions within the network in such a way that, if a certain node is a supply node (it lies in  $\mathcal{N}_p$ ) all edges connected to it are leaving the node and no edge is entering that node. It is always placed as a left end, meaning that the direction of the orientation of the oriented graph points away from the supply node. This makes sense as normally we assume that a supply node is an inlet into the network. All other nodes have at least one arc that ends in them, meaning they are the right node of at least one edge. Furthermore if an arc that is not a pipe ends in a node than no other arc ends in that node. Under Assumption 1 this is always possible (Theorem 1) and creates a DAE of index 1.

## 5 Benchmark Networks

In this section we present four benchmark networks of different complexities. The first benchmark describes a long pipeline, the second benchmark features a small

pipe network including a cycle, the third benchmark has compressor and resistor elements, and the fourth benchmark models a real gas transport network.

### 5.1 Pipeline Benchmark Model

The first benchmark model is taken from [2] and represents a real pipeline. For this pipeline model, with physical specifications given in Table 3, the single pipe model can be utilized together with the scenario, given in Fig. 2, to simulate outputs from inputs. The inputs of the model are the pressure at the inlet of the pipe (the supply node) and the mass-flux at the outlet (the demand node). The outputs are then the mass-flux at the inlet and pressure at the outlet. Starting from a steady state, a scenario is given by the input time series at the inlet and outlet (boundary). In the provided scenario the inlet-pressure is kept constant over time, and the outlet-mass-flux varies over time Fig. 2.

pipeline length	36300m
pipeline diameter	1.422 m
pipeline roughness	0.000015 m
Reynolds number	5000.0
Isothermal speed of sound	$300.0 \frac{\text{m}}{\text{s}}$
Steady supply	84.0 bar
Steady demand	$463.33 \frac{\text{kg}}{\text{s}}$
time horizon	200h

**Table 3** Pipeline benchmark model attributes

We reduced the length of the pipeline to 36.3 km compared to [2] to allow an easier discretization. Practically, the pipeline simulation is realized using 1000 virtual nodes subdividing the long pipeline into a cascade of shorter sequentially connected pipes. The order of the differential equation is then 2000. This refinement strategy, also used in [13], relaxes the Courant-Friedrichs-Levy (CFL) number allowing a stable time-stepping. Using the parameters from Table 3 and the aforementioned input scenario, the resulting output quantities over time are depicted in Fig. 2. These results agree with the behavior described in [2].

### 5.2 Diamond network

This small-scale network is made up of 7 pipes, 1 entry node and 5 exit-nodes. The topology is given by Fig. 3. Note that

$$\mathcal{N}_p = \{u_0\}, \quad \mathcal{N}_q = \{u_1, u_2, u_3, u_4, u_5\}.$$

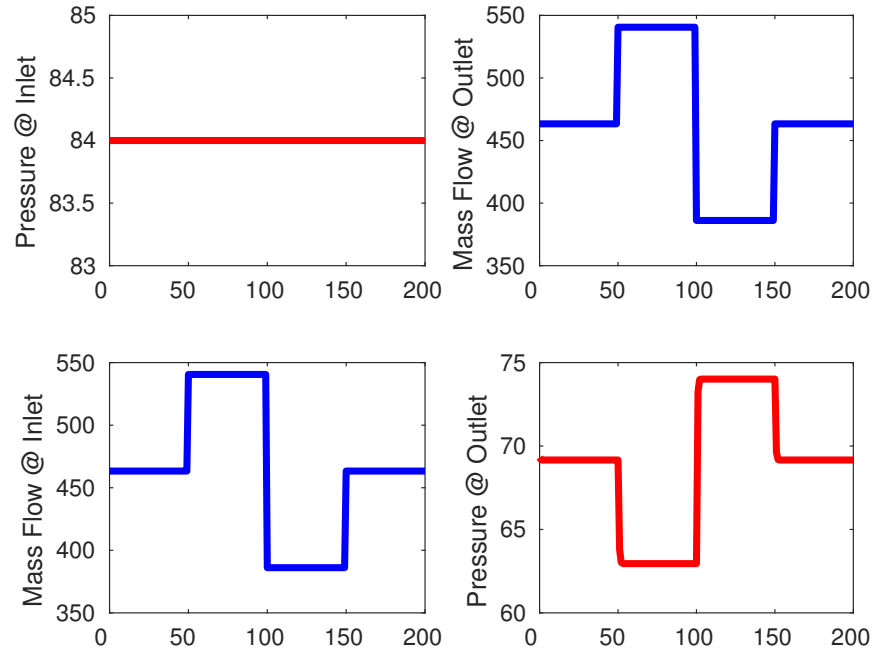


**Fig. 2** Input-Output behavior for the pipeline benchmark. Upper left: Pressure at inlet, upper right: mass flow at outlet, lower left: mass flow at inlet, lower right: pressure at outlet.

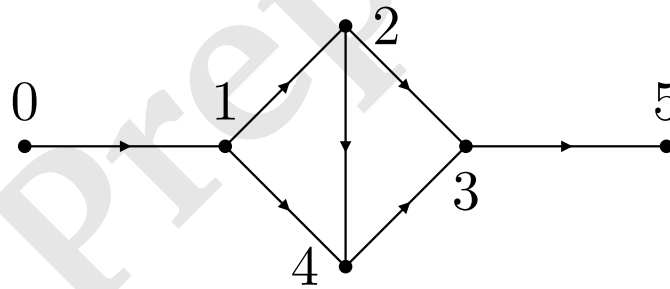


**Fig. 3** *gas\_diamond* – gas transportation network with 6 nodes and 7 arcs.

The gas network *gas\_diamond* (see Fig. 3) contains 6 nodes and 7 pipes. The node  $u_0$  is considered to be a source and is modelled by a (constant) pressure condition of 80bar. The remaining nodes are modelled via flow balance equations, but in our scenario, only at node  $u_6$ , gas will exit the network (see Fig. 4). The demand function is given by a piecewise linear function, with a demand between 80 and 200  $\frac{\text{kg}}{\text{s}}$ . A

graphical representation of a solution to the scenario described in Fig. 4 can be seen in Fig. 5.

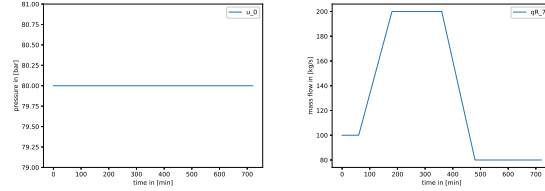


**Fig. 4** (Diamond) pressure curves at the source node  $u_0$  and and demand at sink node  $u_5$ .

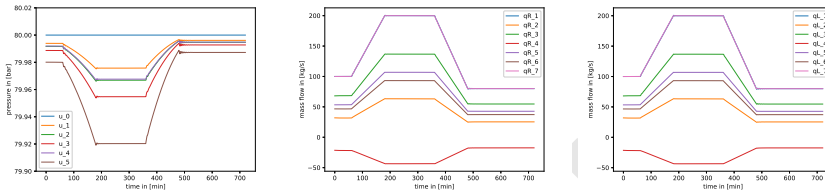


**Fig. 5** (Diamond) Simulation results for scenario in Fig. 4. Pressures at the nodes (left), mass flows at positions  $x = \ell$  (middle) and  $x = 0$  (right) for the pipes.

arc	type	$u$	$v$	(left) flow	right flow	arc	type	$u$	$v$	(left) flow	right flow
$e_0$	pipe	1	0	23	24	$e_{12}$	valve	11	14	47	
$e_1$	pipe	3	2	25	26	$e_{13}$	short pipe	14	15	48	
$e_2$	pipe	5	4	27	28	$e_{14}$	resistor	11	12	49	
$e_3$	pipe	2	1	29	30	$e_{15}$	c.-unit	12	13	50	
$e_4$	pipe	1	6	31	32	$e_{16}$	resistor	13	15	51	
$e_5$	pipe	6	4	33	34	$e_{17}$	pipe	15	16	52	53
$e_6$	pipe	4	2	35	36	$e_{18}$	pipe	16	17	54	55
$e_7$	pipe	6	7	37	38	$e_{19}$	pipe	17	18	56	57
$e_8$	pipe	7	8	39	40	$e_{20}$	pipe	18	19	58	59
$e_9$	pipe	8	9	41	42	$e_{21}$	pipe	19	20	60	61
$e_{10}$	pipe	9	10	43	44	$e_{22}$	pipe	20	21	62	63
$e_{11}$	pipe	10	11	45	46	$e_{23}$	pipe	20	22	64	65

**Table 4** ids of adjacent nodes and flows of edges from *gas\_N23\_A24* network, see Fig. 6.

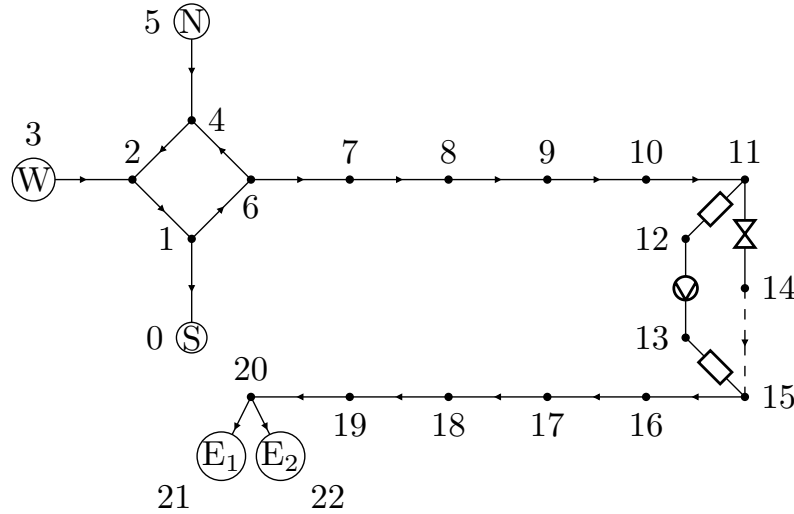


**Fig. 6** *gas\_N23\_A24* – gas transportation network with 23 nodes and 24 arcs. The dashed line represents a short pipe. The node enumeration corresponds to that defined in the benchmark function (for viewing results).

### 5.3 Gas transportation network – *gas\_N23\_A24*

The gas network *gas\_N23\_A24* DAE (see Fig. 6) contains 23 nodes, which can be defined as pressure conditions (mostly at sources) or flow conditions (representing other sources, sinks and innodes) depending on a user definable *behaviour* property. Per default the nodes *N* and *W* are considered to be sources and initialised with pressure conditions. Any other node is considered a flow node, where *S*, *E<sub>1</sub>* and *E<sub>2</sub>* are considered to be the only sinks. Furthermore, a compressor station belongs to the network in the middle of the 100 km pipeline. The station consists of 2 resistors, a by-pass valve, a short pipe and a single idealised compressor unit. The scenario including boundary conditions and target values for the compressor unit is described in an extra file *N23\_A24\_bconditions.xml* as well as implemented or contained within the python script of this benchmark instance *N23\_A24.py*.

Between hour 5 and 7, the compressor unit works maximum power bound and cannot sustain the desired compression ratio until the ingoing pressure raises up again.

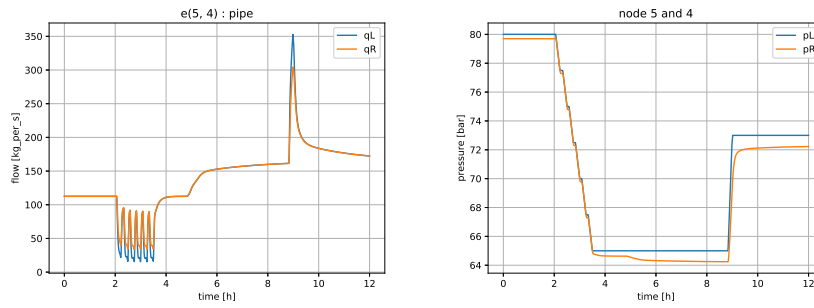


Fig. 7 *gas\_N23\_A24* – pipe  $e_2$  (node 4 & source node  $N$ ): flow and pressure curves

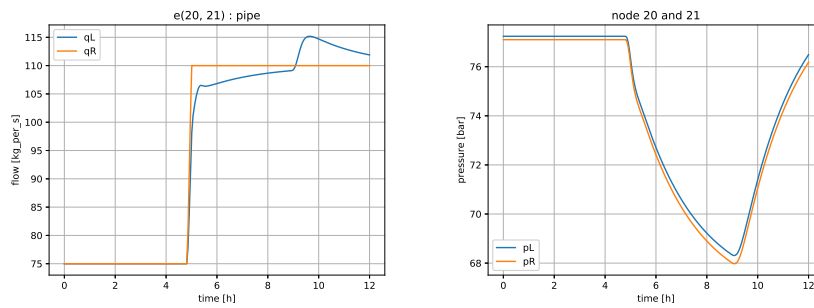


Fig. 8 *gas\_N23\_A24* – pipe  $e_{22}$  (node 20 & exit node  $E_1$ ): flow and pressure curves

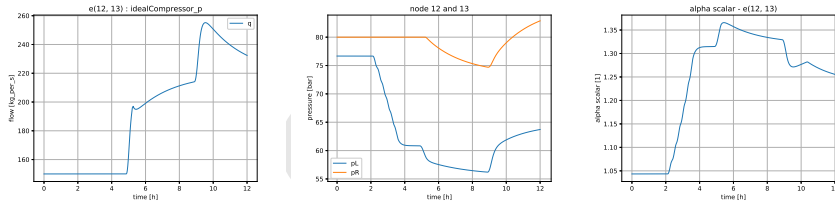
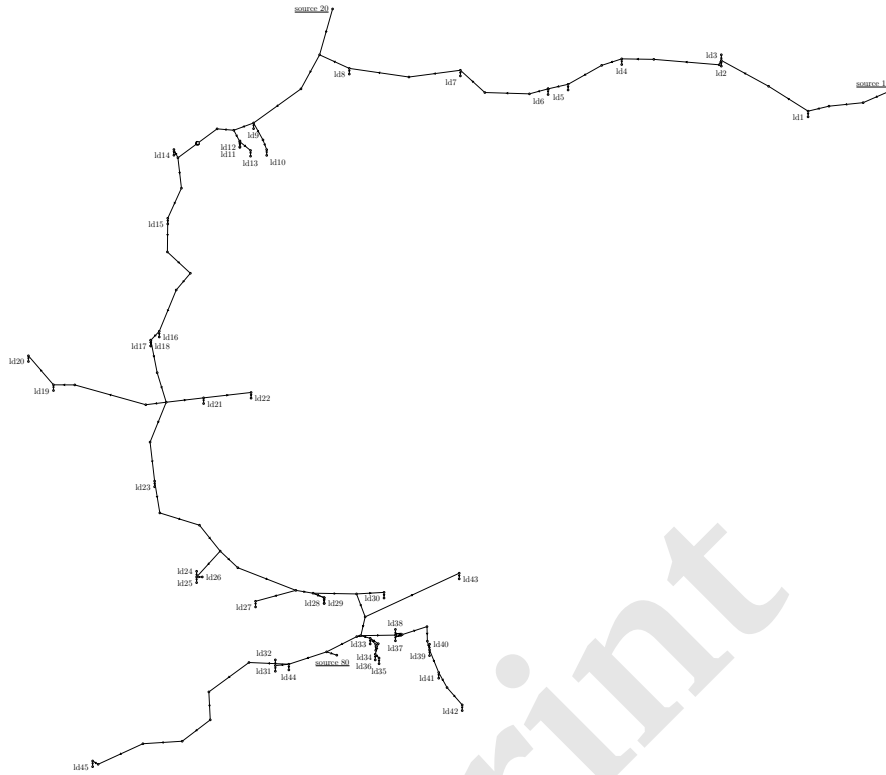


Fig. 9 *gas\_N23\_A24* – idealised compressor unit (nodes 12 & 13): flow, pressures and compression-factor ( $\alpha$ )

### 5.4 Gas transportation network – *gas\_N138\_A139* (derived from *GasLib-134*)

The gas network *gas\_N138\_A139* DAE (see Fig. 10) contains 138 nodes and is derived from the stationary gas network instance *GasLib-134* (see [16] and [27]). Here the compressor station and the control valve from the original source are extended by an ingoing and outgoing resistor as well as a bypass valve. To that end 4 additional nodes were introduced increasing the number from 134 up to 138. The rest



**Fig. 10** *gaslib\_134* – gas network from *gaslib.zib.de* with 134 nodes and 133 arcs. The node IDs of all 45 sinks and the 3 sources are displayed.

of the network topology stays the same. All nodes and arcs in the python implementation of this benchmark example are enumerated and do have a name property, too. This example contains an idealized compressor unit and a control valve. The 6 hour transient scenario was created on the basis of the daily nominations from the *GasLib-134* instance in that the nominated flows are interpolated piece-wise linear and switched through every 2 hours.

Between hour 2 and 6 the source node with name *node\_1* stops providing gas to the network (see Fig. 11). The adjacent pipe with name *p\_br1* is 14.56 km long such that gas can still be drawn from the other side while the gas pressure and so the gas density decreases. It can be observed that the compressor station (see Fig. 13) increases its power or the compression ratio  $\alpha$  resp. as a counter reaction to preserve the outgoing target pressure which is set to  $p_{r,\text{set}} \equiv 70$  bar.

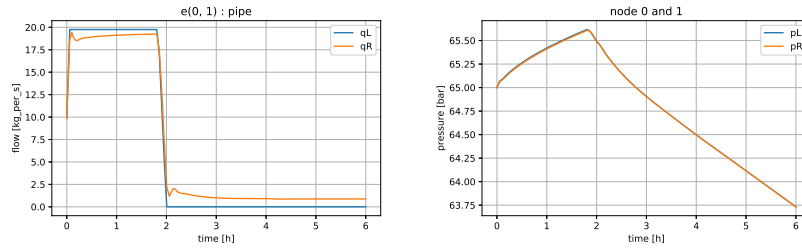


**Fig. 11** *gas\_N138\_A139* – pipe *p.br1* (connecting the source node (name: *node\_1*, idx: 0) with innode (name: *node\_2*, idx: 1): flow and pressure curves

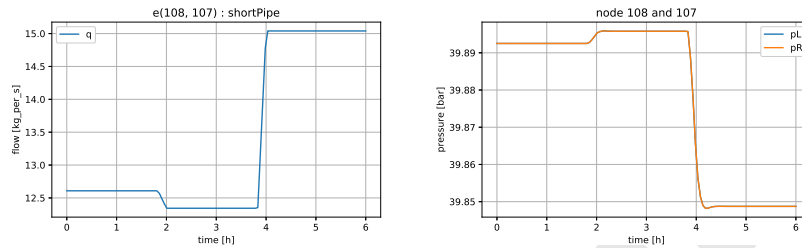


**Fig. 12** *gas\_N138\_A139* – pipe *node\_72\_ld42* (connecting the innode (name: *node\_72*, idx: 108) with sink node (name: *node\_ld42*, idx: 107): flow and pressure curves

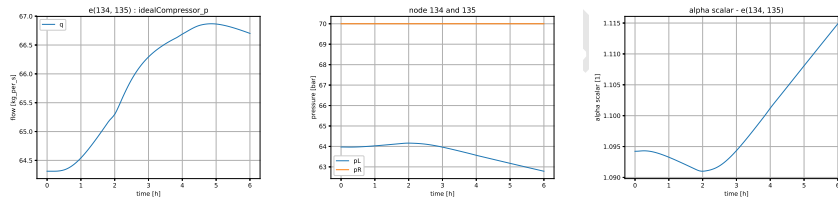


**Fig. 13** *gas\_N138\_A139* – idealised compressor unit (nodes 134 & 135): flow, pressures and compression-factor ( $\alpha$ )

## 6 Concluding Remarks

Gas network modelling and numerical solution thereof is at the interface between the real life application and differential algebraic equation research, This is also an interesting class of applications due to their manifold challenges, such as nonlinearity or hyperbolicity. In this work we presented a modular gas network model as well as four benchmarks, which enable testing of extensions of this basic model as well as implementations of DAE solvers.

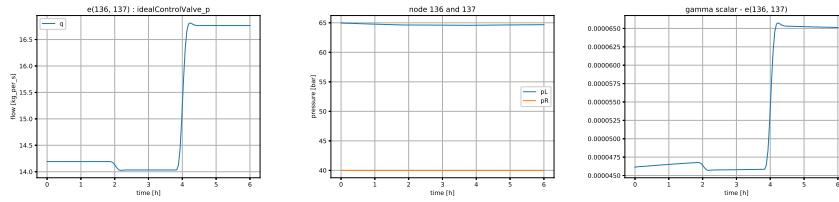


**Fig. 14** *gas\_N138\_A139* – control valves (nodes 136 & 137): flow, pressures and degree of openness ( $\alpha$ )

## Code and Data Availability

The code and data used in this work can be obtained as supplementary material. The data is prepared in form of three XML-files for each benchmark example. The *net.xml*-file containing the network topology, the *bconditions.xml*-file providing the boundary conditions (i.e. the in- and out going flows at sources and sinks as well as fixed pressures and target values for compressors and control valves) and the *result.xml*-file containing our reference solution. XML Schema or *XSD* files for the validation and documentation will be provided alongside. These schema files were created to store transient gas network scenarios and were kindly supplied to us by the SFB Transregio 154 (homepage <http://trr154.fau.de/index.php/en/>). It should be noted, however that the *net.xml* and the *bconditions.xml* files of both the *gas\_N23\_A24* and the *gas\_N138\_A139* will not completely validate against the schemes. The formats were intended for a more detailed description of compressor units as so called turbo compressors. In this paper we introduced an idealized description of compressors which are not covered by the schema files. Besides this described data the supplementary material also includes code that creates the Differential Algebraic Equation for each of this networks. For the pipeline this is done in MATLAB, and for the others it is done in Python.

### Acknowledgements

Supported by the German Federal Ministry for Economic Affairs and Energy, in the joint project: “**MathEnergy** – Mathematical Key Technologies for Evolving Energy Grids”, sub-project: Model Order Reduction (Grant number: 0324019B).

The work for the article has been conducted within the Research Campus MODAL funded by the German Federal Ministry of Education and Research (BMBF) (fund number 05M14ZAM).

We also acknowledge funding through the DFG CRC/Transregio 154 “Mathematical Modelling, Simulation and Optimization using the Example of Gas Networks”, Subproject C02

### References

1. T.-P. Azevedo-Perdicoulis and G. Jank. Modelling aspects of describing a gas network through a DAE system. In *Proceedings of the 3rd IFAC Symposium on System Structure and Control*, volume 40(20), pages 40–45, 2007. doi:10.3182/20071017-3-BR-2923.00007.
2. M. Chaczykowski. Sensitivity of pipeline gas flow model to the selection of the equation of state. *Chemical Engineering Research and Design*, 87:1596–1603, 2009. doi:10.1016/j.cherd.2009.06.008.
3. I. J. Chodanovich and G. E. Odisharija. Analiz žavisimosti dlja koefizienta gidravličeskogo soprotivlenija (analysis of the dependency of the pipe friction factor). *Gažovaja Promyshlennost*, 9(11):38–42, 1964.
4. C. F. Colebrook. Turbulent flows in pipes, with particular reference to the transition region between smooth and rough pipe laws. *Journal of the Institute of Civil Engineering*, 11:133–156, 1939.
5. P. Domschke, B. Geißler, O. Kolb, J. Lang, A. Martin, and A. Morsi. Combination of nonlinear and linear optimization of transient gas networks. *INFORMS Journal on Computing*, 23(4):605–617, 2011. doi:10.1287/ijoc.1100.0429.
6. S. Dymkou, G. Leugering, and G. Jank. Repetitive processes modelling of gas transport networks. In *2007 International Workshop on Multidimensional (nD) Systems*, pages 101–108, 2007. doi:10.1109/NDS.2007.4509556.
7. K. Ehrhardt and M. C. Steinbach. Nonlinear optimization in gas networks. In H. G. Bock, H. X. Phu, E. Kostina, and R. Rannacher, editors, *Modeling, Simulation and Optimization of Complex Processes*, Proceedings of the International Conference on High Performance Scientific Computing, pages 139–148. Springer, 2005. doi:10.1007/3-540-27170-8\_11.
8. A. Fügenschuh, B. Geißler, R. Gollmer, A. Morsi, M. E. Pfetsch, J. Rövekamp, M. Schmidt, K. Spreckelsen, and M. C. Steinbach. Chapter 2: Physical and technical fundamentals of gas networks. In T. Koch, B. Hiller, M. E. Pfetsch, and L. Schewe, editors, *Evaluating Gas Network Capacities*, MOS-SIAM Series on Optimization, pages 17–43. SIAM, 2015. doi:10.1137/1.9781611973693.ch2.
9. S. Grundel, N. Hornung, B. Klaassen, P. Benner, and T. Clees. Computing surrogates for gas network simulation using model order reduction. In *Surrogate-Based Modeling and Optimization, Applications in Engineering*, pages 189–212. Springer, 2013. doi:10.1007/978-1-4614-7551-4\_9.
10. S. Grundel, N. Hornung, and S. Roggendorf. Numerical aspects of model order reduction for gas transportation networks. In *Simulation-Driven Modeling and Optimization*, volume 153 of *Proceedings in Mathematics & Statistics*, pages 1–28. Springer, 2016. doi:10.1007/978-3-319-27517-8\_1.
11. S. Grundel, L. Jansen, N. Hornung, T. Clees, C. Tischendorf, and P. Benner. Model order reduction of differential algebraic equations arising from the simulation of gas transport networks. In *Progress in Differential-Algebraic Equations*, Differential-Algebraic Equations Forum, pages 183–205. Springer, 2014. doi:10.1007/978-3-662-44926-4\_9.

12. M. Herty. Modeling, simulation and optimization of gas networks with compressors. *Networks and Heterogenous Media*, 2(1):81–97, 2007. doi:10.3934/nhm.2007.2.81.
13. M. Herty, J. Mohring, and V. Sachers. A new model for gas flow in pipe networks. *Mathematical Methods in the Applied Sciences*, 33:845–855, 2010. doi:10.1002/mma.1197.
14. P. Hofer. Beurteilung von Fehlern in Rohrnetzberechnungen (Error evaluation in calculation of pipelines). *GWF–Gas/Erdgas*, 114(3):113–119, 1973.
15. C. Huck and C. Tischendorf. Topology motivated discretization of hyperbolic PDAEs describing flow networks. 2017. URL: <https://opus4.kobv.de/opus4-trr154/frontdoor/index/index/docId/137>.
16. J. Humpola, I. Joormann, N. Kanelakis, D. Oucherif, M. E. Pfetsch, L. Schewe, M. Schmidt, R. Schwarz, and M. Sirvent. GasLib – A Library of Gas Network Instances. Technical report, Mathematical Optimization Society, 2017. URL: [http://www.optimization-online.org/DB\\_HTML/2015/11/5216.html](http://www.optimization-online.org/DB_HTML/2015/11/5216.html).
17. J. Králik, P. Stiegler, Z. Vostrý, and J. Závorka. *Dynamic Modeling of Large-Scale Networks with Application to Gas Distribution*, volume 6 of *Automation and Control*. Elsevier, New York, 1988.
18. R. J. LeVeque. Nonlinear conservation laws and finite volume methods. In O. Steiner and A. Gautschy, editors, *Computational Methods for Astrophysical Fluid Flow*, volume 27 of *Saas-Fee Advanced Courses*, pages 1–159. Springer Berlin, Heidelberg, 1997. doi:10.1007/3-540-31632-9\_1.
19. LIWACOM Informationstechnik GmbH and SIMONE research group s. r. o., Essen. *SIMONE Software. Gleichungen und Methoden.*, 2004.
20. J. Mischner, H. G. Fasold, and J. Heymer, editors. *gas2energy.net*. Edition gas for energy. DIV, 2016. URL: <https://www.di-verlag.de/de/gas2energy.net2>.
21. S. Moritz. *A Mixed Integer Approach for the Transient Case of Gas Network Optimization*. PhD thesis, Technische Universität, Darmstadt, 2007. URL: <http://tuprints.ulb.tu-darmstadt.de/785/>.
22. B. Nekrasov. *Hydraulics for Aeronautical Engineers*. Peace Publishers, 1969. URL: <https://archive.org/details/in.ernet.dli.2015.85993>.
23. J. Nikuradse. Gesetzmäßigkeiten der turbulenten Strömung in glatten Röhren. *VDI-Forschungsheft*, 356:1–36, 1932.
24. A. Osiadacz. Simulation of transient gas flows in networks. *International Journal for Numerical Methods in Fluids*, 4:13–24, 1984. doi:10.1002/flid.1650040103.
25. A. J. Osiadacz and M. Chaczykowski. Verification of transient gas flow simulation model. In *PSIG Annual Meeting*, pages 1–10, 2010. URL: <https://www.onepetro.org/conference-paper/PSIG-1010>.
26. J. Papay. *A Termelestechnologiai Parameterek Valtozasa a Gazleplek Muvelese Soran*, pages 267–273. Tud. Kuzl., 1968.
27. Marc. E Pfetsch, Armin Fügenschuh, Björn Geißler, Nina Geißler, Ralf Gollmer, Benjamin Hiller, Jesco Humpola, Thorsten Koch, Thomas Lehmann, Alexander Martin, Antonio Morsi, Jessica Rövekamp, Lars Schewe, Martin Schmidt, Rüdiger Schultz, Robert Schwarz, Jonas Schweiger, Claudia Stangl, Marc C. Steinbach, Stefan Vigerske, and Bernhard M. Willert. Validation of nominations in gas network optimization: Models, methods, and solutions. *Optimization Methods and Software*, 2014. doi:10.1080/10556788.2014.888426.
28. T. van der Hoeven. *Math in Gas and the art of linearization*. PhD thesis, University of Groningen, 2004. URL: <http://hdl.handle.net/11370/0bbb8138-6d96-4d79-aac3-e46983d1fd33>.
29. D. J. Zigrang and N. D. Sylvester. A review of explicit friction factor equations. *Journal of Energy Resources Technology*, 107(2):280–283, 1985. doi:10.1115/1.3231190.